Analysis of a local defect correction approach on composite grids

EINDHOVEN UNIVERSITY OF TECHNOLOGY
Department of Mathematics and Computing Science

RANA 94-09
June 1994

Analysis of a Local Defect Correction Approach on Composite Grids

by

P.J.J. Ferket

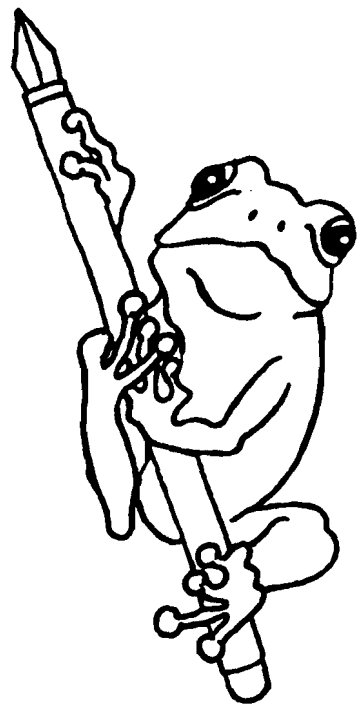

Reports on Applied and Numerical Analysis
Department of Mathematics and Computing Science
Eindhoven University of Technology
P.O. Box 513
5600 MB Eindhoven
The Netherlands
ISSN: 0926–4507

Analysis of a Local Defect Correction Approach on Composite Grids

P.J.J. Ferket

Eindhoven University of Technology,
Department of Mathematics and Computing Science,
P.O. Box 513, 5600 MB Eindhoven, The Netherlands.

Abstract

In this paper we consider the problem of discretization on a composite grid that consists of a global uniform coarse grid and a local uniform fine grid. For elliptic problems a local defect correction approach is described. The error of the resulting approximation is analysed. It follows that in general the accuracy of this approximation is (much) better than the accuracy of an approximation that results from an approach without local defect correction. The use of a "buffer zone" in the local defect correction approach appears to be essential for several problems. We discuss when such a "buffer zone" is necessary to obtain satisfactory results.

A.M.S. Classifications: 65N06, 65N50
Keywords : Local uniform grid refinement, local defect correction, error analysis.

1 Introduction

Many practical *boundary value problems* produce solutions that contain several *high activity regions.* In these regions the solution varies much more rapidly than in the remaining part of the domain. This behaviour of the solution may be caused by the differential operator itself, by the forcing term in the differential equation, by the boundary conditions or by an irregular boundary (e.g. a re-entrant corner).

Boundary value problems that produce such solutions can be found, for example, in the field of combustion. All variables that occur in the combustion process have sharp gradients *inside* the flame (which usually is only a small part of the region of interest). *Outside* the flame they are nearly constant. In Figure 1 typical temperature, mass fraction and reaction rate profiles across a planar flame are shown (cf. [7]).

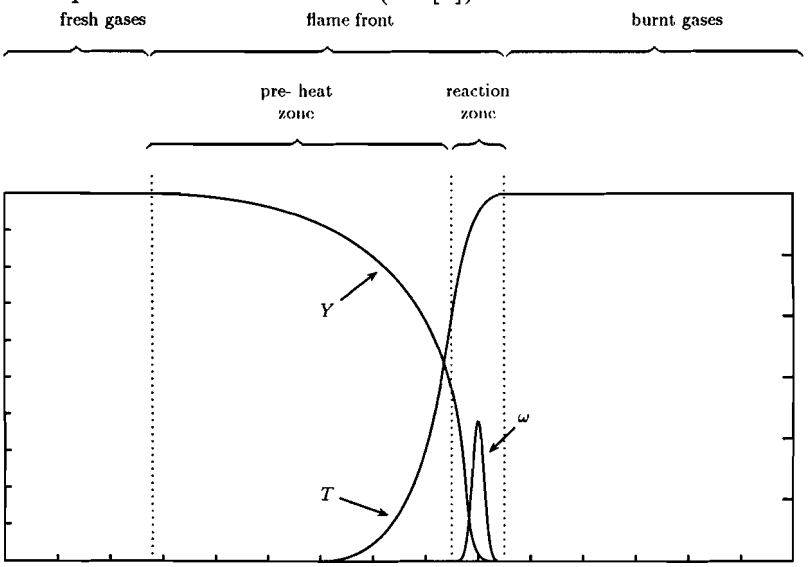

Figure 1: Temperature (T), mass fraction (Y), and reaction rate (ω) across a planar flame.

In order to obtain a numerical approximation of the solution, the boundary value problem can be discretized on a *uniform grid.* The accuracy of the numerical approximation depends, among other things, on the grid size. Due to the large variations of the solution in the high activity regions, a relatively small grid size is required there to obtain a sufficiently accurate approximation of the solution. Outside the high activity regions the behaviour of the solution is much more smooth. Therefore a (much) larger grid size seems to be sufficient in that part of the domain. However, if we discretize on a uniform grid, the grid size is small everywhere. Inside the high activity regions this grid size is in agreement with the behaviour of the continuous solution, but outside these regions it is not. Because of the large number of grid points in the uniform grid, the system of algebraic equations that results from the discretization process will be relatively large. Furthermore, the numerical approximation has to be stored at each grid point. So it is clear that approximating the continuous solution on a single uniform grid is *computationally inefficient* for boundary value problems that produce solutions that contain small high activity regions.

Instead, the solution can be approximated using *several uniform grids with different grid sizes that cover different parts of the domain.* At least one grid should cover the entire domain. The grid size of this *global coarse grid* is chosen in agreement with the smooth behaviour of the

solution outside the high activity regions. Besides a global grid several *local grids* are used that are uniform too. Each of them covers only a (small) part of the domain and contains a high activity region. The grid size of each of these grids is chosen in agreement with the behaviour of the solution in the corresponding high activity region. In this way every part of the domain is covered by a (locally) uniform grid whose grid size is in agreement with the behaviour of the continuous solution in that part of the domain. This refinement strategy is known as *local uniform grid refinement* (see e.g. [10], [11]). The solution is approximated on a *composite grid* which is the union of uniform subgrids. Other approaches use a *truly nonuniform* grid (e.g. nonuniform finite element meshes). Some advantages of using a composite grid are relatively simple data structures, accurate discretization capabilities, and the existence of very efficient solvers for uniform grids.

There are several ways of approximating the continuous solution on a composite grid. In *FAC-methods* ([10]) the partial differential equation is discretized and solved on the composite grid (which is nonuniform), but the uniform subgrids are where all of the actual computation takes place. In the *local defect correction method* ([5]) the partial differential equation is discretized and solved only on the uniform subgrids and not on the composite grid. The local defect correction method is an iterative discretization method. At every step discrete problems with respect to all uniform subgrids are defined and solved. The approximations on the subgrids generate an approximation of the continuous solution on the composite grid.

If the number of local defect correction iterations that is necessary to compute a satisfactory approximation is large, then the number of grid points that is involved in this iterative discretization process may be larger than the number of grid points in a corresponding global fine grid. Numerical examples (see e.g. [5]) indicate that the iterates in the local defect correction method converge very fast. Moreover the limit value of this iterative process is a satisfactory approximation of the continuous solution: its accuracy is comparable to the accuracy of a corresponding global fine grid problem. Therefore it is interesting to consider *the approximation that results after one step of the local defect correction iteration* in [5]. An analysis of this approximation is given in this paper. This error analysis results in a clear insight into the accuracy of this approximation. Special attention is paid to the role of some "buffer zone" in the local regions. From the error analysis it becomes clear when such a buffer zone is necessary to obtain satisfactory results.

The remainder of this paper is organized as follows. In Section 2 the model situation is described and some notational aspects are introduced. In Section 3 we consider a discretization process *without* local defect correction. First the boundary value problem is discretized with respect to the global coarse grid; then the boundary value problem is discretized with respect to each local fine grid. The solution of the global coarse grid problem is used to *impose Dirichlet boundary conditions on the interfaces between the local regions and the remainder of the domain.* It is shown that in general the accuracy of the approximation that results from this discretization process is not in agreement with the grid sizes that are used. In Section 4 the local defect correction approach is described. This approach is an extension of the approach from Section 3. After solving the discrete local problems, we return to the global coarse grid and adapt the right hand side of the global coarse grid problem. The approximation that results from this new global problem is used to impose Dirichlet boundary conditions on the interfaces between the local regions and the remainder of the domain. The error in the resulting approximation on the composite grid is analysed and discussed. The effect of the local defect correction approach is also shown by several numerical examples.

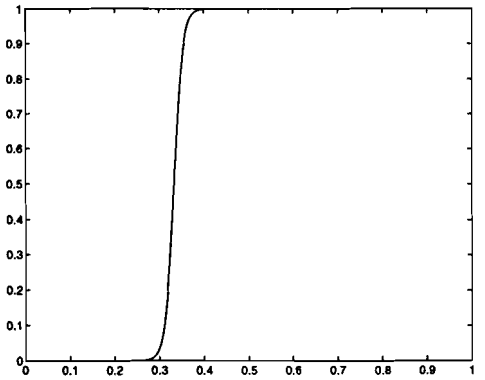

Figure 2: Continuous solution U in (2.3) with $A = 50$ and $z = 0.333$.

2 Description of the Model Situation

In this paper we consider a *Dirichlet boundary value problem*

$$\begin{aligned} \mathcal{L}U &= f \quad \text{in } \Omega, \\ U &= g \quad \text{at } \partial\Omega. \end{aligned} \tag{2.1}$$

We assume that $\Omega = (0,1)$ in the one dimensional case and $\Omega = (0,1) \times (0,1)$ in the two dimensional case; $\partial\Omega$ is the boundary of Ω and $\mathcal{L}$ is a scalar, linear, elliptic, second-order differential operator. We assume that the solution U of (2.1) contains *one high activity region.* Inside the high activity region the solution U varies much more rapidly than outside this region. We assume that this behaviour of U is induced by the right hand side f in the partial differential equation or by the right hand side g in the Dirichlet boundary condition.

Example 2.1
Consider the one dimensional Poisson problem

$$\begin{aligned} -U_{xx} &= f(x) \quad 0 < x < 1, \\ U(0) &= a, \\ U(1) &= b. \end{aligned} \tag{2.2}$$

If the right hand side f is given by

$$f(x) = A^2 \frac{\tanh(A(x-z))}{\cosh^2(A(x-z))},$$

and if

$$a = (\tanh(-Az) + 1)/2, \quad b = (\tanh(A(1-z)) + 1)/2,$$

then the continuous solution is given by

$$U(x) = (\tanh(A(x-z)) + 1)/2. \tag{2.3}$$

In Figure 2 this function is shown for $A = 50$ and $z = 0.333$.
We see that U varies very rapidly in a small region around x and that it is nearly constant outside this region. □

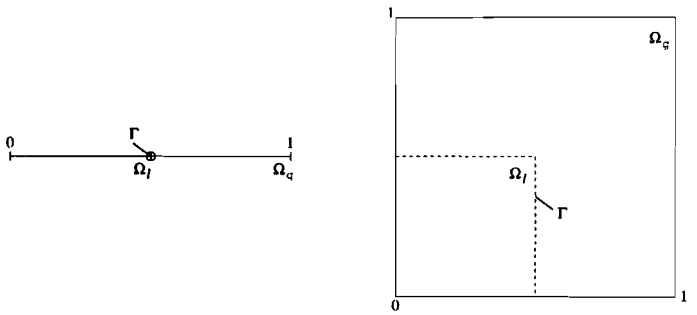

Figure 3: Examples of Ω, Ω_l and Γ in $\mathbb{R}^1$ and $\mathbb{R}^2$.

In order to obtain a numerical approximation of U we discretize (2.1) with respect to a uniform global grid with grid size h. This uniform grid is called the *global fine grid* and we denote it by Ω^h. Finite difference discretization yields the *global fine grid problem*:

$$L^h u^h = f^h. \tag{2.4}$$

Here u^h and f^h are grid functions on Ω^h. The Dirichlet boundary conditions of (2.1) are incorporated in f^h. If we substitute U in (2.4) we obtain the *local discretization error vector* of this discrete problem:

$$d^h := L^h U^h - f^h. \tag{2.5}$$

In (2.5) U^h is the restriction of U to Ω^h. In the remainder we use a similar notation for restrictions of U to other grids. At each grid point $\mathbf{x} \in \Omega^h$ we have

$$d^h(\mathbf{x}) = c(\mathbf{x}, h)h^\kappa, \tag{2.6}$$

with κ the order of consistency of the finite difference scheme that is used. We assume that the same finite difference scheme is used at all grid points. The factor $c(\mathbf{x}, h)$ depends on higher order derivatives of U in the neighbourhood of $\mathbf{x}$ (see Example 2.2). Since U varies much more rapidly inside the high activity region than in the remainder of the domain, it is clear that $|d^h(\mathbf{x})|$ is much larger at several grid points inside or near the high activity region than at grid points away from this region.

Example 2.2
If we discretize the one dimensional Poisson problem (2.2) using the central difference scheme on a uniform grid with grid size h we get

$$d^h(\mathbf{x}) = -\frac{1}{24}(U^{(4)}(x - \xi_- h) + U^{(4)}(x + \xi_+ h))h^2$$

with $0 < \xi_-, \xi_+ < 1$. We see that $c(x, h)$ depends on fourth order derivatives of U in this case.

□

Combination of (2.4) and (2.5) yields

$$L^h(U^h - u^h) = d^h. \tag{2.7}$$

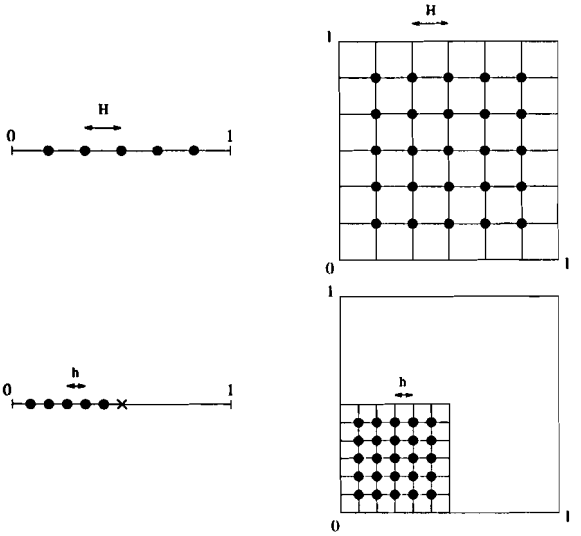

Figure 4: Examples of global coarse grids Ω^H and local fine grids Ω_l^h in $\mathbb{R}^1$ and $\mathbb{R}^2$.

If L^h is nonsingular, then the error vector $U^h - u^h$ is given by

$$U^h - u^h = (L^h)^{-1} d^h. \tag{2.8}$$

So the error vector $U^h - u^h$ depends on the local discretization error vector d^h and on the inverse operator $(L^h)^{-1}$. We have seen that some compononts of $|d^h|$ are much larger than others. The error $\|U^h - u^h\|_\infty$ is determined by these large components of the local discretization error vector. Suppose that the grid size h is such that

$$\|U^h - u^h\|_\infty \approx TOL.$$

Then for this tolerance criterium the grid size h is in agreement with the behaviour of the continuous solution *inside the high activity region.* However, *outside the high activity region* the continuous solution behaves much more smoothly and such a fine resolution is not needed there.

Now we introduce a local region Ω_l that satisfies the following four conditions:

1. $\Omega_l \subset \Omega$,
2. the high activity region is contained in Ω_l,
3. near the boundary $\partial\Omega_l$ the continuous solution varies smoothly,
4. Ω_l is a "small" extension of the high activity region.

Some part of $\partial\Omega_l$ may coincide with $\partial\Omega$. The remaining part forms the *interface* Γ between Ω_l and Ω (see Figure 3).

In the following sections we consider discretization processes that use a *global coarse grid* Ω^H and a *local fine grid* Ω_l^h. The global coarse grid Ω^H is a uniform grid with grid size H, $H > h$, that covers the entire domain. The local fine grid Ω_l^h is a uniform grid with grid size h that covers the region Ω_l only (see Figure 4). The ratio of H and h is called the *refinement*

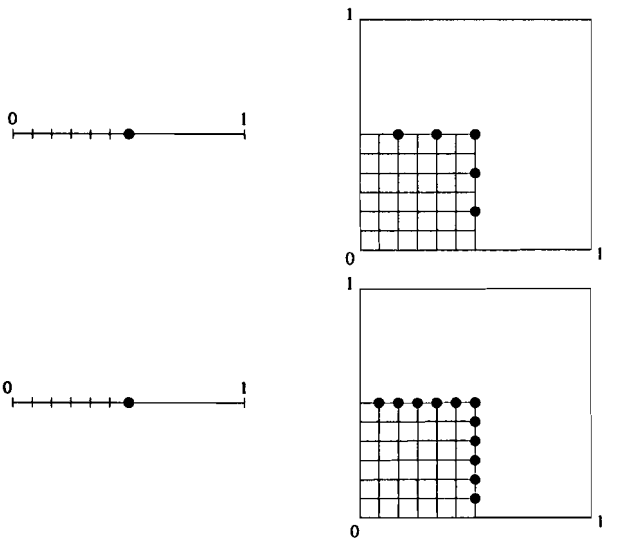

Figure 5: Examples of coarse interface grids Γ^H and fine interface grids Γ^h in $\mathbb{R}^1$ and $\mathbb{R}^2$.

factor $\rho := H/h$. We note that Ω_l^h does not contain grid points on the interface. We assume that the interface Γ coincides with grid points of Ω^H in the one dimensional case and with grid lines of Ω^H in the two dimensional case. Then we can introduce the *coarse interface grid* $\Gamma^H = \Gamma \cap \Omega^H$ and the *fine interface grid* $\Gamma^h = \Gamma \cap \Omega^h$ (see Figure 5). In the one dimensional case we have that $\Gamma^h = \Gamma^H$, while in the two dimensional case $\Gamma^H \subset \Gamma^h$.

Finite difference discretization of (2.1) with respect to Ω^H yields the *global coarse grid problem*

$$L^H u^H = f^H. \tag{2.9}$$

One can use the same finite difference approximation formula as when discretizing on the global fine grid. However, this is not essential. The theory also applies when (2.4) and (2.9) correspond to different finite difference approximation formulas. The local discretization error vector of the global coarse grid problem is given by

$$d^H := L^H U^H - f^H. \tag{2.10}$$

Similarly as for $|d^h|$, we have that $|d^H|$ is much larger at several grid points inside or near the high activity region than at grid points away from this region: $\|d^H\|_{\infty,\Omega^H\setminus\Omega_l} \ll \|d^H\|_\infty$. ($\|d^H\|_{\infty,\Omega^H\setminus\Omega_l} = \max_{\mathbf{x}\in\Omega^H\setminus\Omega_l} |d^H(\mathbf{x})|$). In the remainder it is assumed that the grid size H and the local region Ω_l are such that

$$\max_{\mathbf{x}\in\Omega^H\setminus\Omega_l} |d^H(\mathbf{x})| \approx \max_{\mathbf{x}\in\Omega^h} |d^h(\mathbf{x})|. \tag{2.11}$$

Relation (2.11) is a specification of the statement that the grid sizes h and H are in agreement with the behaviour of the continuous solution inside, respectively outside the high activity region. For the problems under consideration here we have $h \ll H$. Relation (2.11) is reasonable when H is not "too large" (the high activity region must contain several grid points of Ω^H) and Ω_l is not "too small" (several grid points of Ω^H must lie inside Ω_l but outside the high activity regioin).

In the following sections we consider discretization processes that make use of the global coarse grid Ω^H and the local fine grid Ω_l^h. As a result we get approximations of the continuous solution U on the *composite grid* $\Omega^c = \Omega^H \cup \Omega_l^h$.

3 A Discretization Approach Without Local Defect Correction

We start by discretizing (2.1) on the global coarse grid Ω^H. The resulting global coarse grid problem is given by

$$L^H u^H = f^H. \tag{3.1}$$

In (3.1) u^H and f^H are grid functions on Ω^H. Next we discretize (2.1) with respect to the local fine grid Ω_l^h. We have to define Dirichlet boundary conditions at all grid points of Γ^h. Therefore, we restrict the solution of (3.1) to the coarse interface grid Γ^H:

$$(r_\Gamma u^H)(\mathbf{x}) = u^H(\mathbf{x}) \quad \mathbf{x} \in \Gamma^H. \tag{3.2}$$

In (3.2) r_Γ is a *trivial injection* that restricts grid functions on Ω^H to Γ^H. This trivial injection yields Dirichlet boundary conditions at all grid points $\mathbf{x} \in \Gamma^H$. Dirichlet boundary conditions at grid points $\mathbf{x} \in \Gamma^h \backslash \Gamma^H$ result from interpolating these values. We note that this interpolation can be omitted in the one dimensional case, since then $\Gamma^H = \Gamma^h$. The resulting *local fine grid problem* is given by

$$L_l^h u_l^h = f_l^h - L_\Gamma^h p_\Gamma r_\Gamma u^H. \tag{3.3}$$

In (3.3) u_l^h and f_l^h are grid functions on Ω_l^h. *Natural* Dirichlet boundary conditions on $\partial\Omega_l \cap \partial\Omega$ are incorporated into f_l^h. The incorporation of the *artificial* Dirichlet boundary conditions on Γ is given explicitly by the term $-L_\Gamma^h p_\Gamma r_\Gamma u^H$ (see Example 3.1). In this term p_Γ is an *interpolation operator* that prolongates grid functions on Γ^H to Γ^h. In the one dimensional case p_Γ is the identity operator on Γ^H. In this discretization process on the local fine grid we use the same finite difference scheme as in the discretization process on the global fine grid:

$$L^h w^h(\mathbf{x}) = L_l^h w_l^h(\mathbf{x}) + L_\Gamma^h w_\Gamma^h(\mathbf{x}) \quad \mathbf{x} \in \Omega_l^h,$$

for all w^h, w_l^h, and w_Γ^h with

$$\begin{aligned} w_l^h(\mathbf{x}) &= w^h(\mathbf{x}) \quad \mathbf{x} \in \Omega_l^h, \\ w_\Gamma^h(\mathbf{x}) &= w^h(\mathbf{x}) \quad \mathbf{x} \in \Gamma^h. \end{aligned}$$

Example 3.1
Consider the one dimensional Poisson problem (2.2):

$$\begin{aligned} -U_{xx} &= f(x) \quad 0 < x < 1, \\ U(0) &= a, \\ U(1) &= b. \end{aligned}$$

Suppose that $H = 1/8$, $\Omega_l = (0, 1/4)$, and $h = 1/32$.
Define

$$\begin{aligned} x_i &:= i * H \quad i = 1, \ldots, 7, \\ y_j &:= j * h \quad j = 1, \ldots, 7. \end{aligned}$$

If we use central differences we get the following local fine grid problem

$$\frac{1}{h^2}\begin{pmatrix} 2 & -1 & & & \\ -1 & 2 & -1 & & \\ & & \ddots & & \\ & & -1 & 2 & -1 \\ & & & -1 & 2 \end{pmatrix}\begin{pmatrix} u_l^h(y_1) \\ \\ \vdots \\ \\ u_l^h(y_7) \end{pmatrix} = \begin{pmatrix} f(y_1)+\frac{a}{h^2} \\ f(y_2) \\ \vdots \\ \\ f(y_7) \end{pmatrix} - \frac{1}{h^2}\begin{pmatrix} 0 \\ 0 \\ \vdots \\ 0 \\ -1 \end{pmatrix} u^H(x_2) \quad \square$$

From this discretization process the following approximation on the composite grid $\Omega^c = \Omega^H \cup \Omega_l^h$ results:

$$u^c(\mathbf{x}) := \begin{cases} u_l^h(\mathbf{x}) & \mathbf{x} \in \Omega_l^h \\ u^H(\mathbf{x}) & \mathbf{x} \in \Omega^c \backslash \Omega_l^h \end{cases} . \tag{3.4}$$

It is clear that the accuracy of this approximation depends on the accuracy of the global coarse grid approximation u^H at grid points outside Ω_l and on the accuracy of the local fine grid approximation u_l^h at grid points inside Ω_l. We have the following expressions for the error vectors $U^H - u^H$ and $U_l^h - u_l^h$.

Theorem 3.2
The approximation u^H satisfies

$$L^H(U^H - u^H) = d^H. \tag{3.5}$$

with d^H as in (2.10).
Proof:
Combination of (2.9) and (2.10) yields (3.5). $\square$

Theorem 3.3
The approximation u_l^h that results from (3.3) satisfies

$$L_l^h(U_l^h - u_l^h) = d_l^h + L_\Gamma^h(p_\Gamma U_\Gamma^H - U_\Gamma^h) - L_\Gamma^h p_\Gamma r_\Gamma (U^H - u^H), \tag{3.6}$$

with

$$d_l^h(\mathbf{x}) = d^h(\mathbf{x}) \quad \mathbf{x} \in \Omega_l^h \tag{3.7}$$

and d^h as in (2.5).
Proof:
Since the same finite difference approximations are used in the discretization process on the local fine grid as on the global fine grid we have that

$$L_l^h U_l^h = f_l^h - L_\Gamma^h U_\Gamma^h + d_l^h$$

with

$$d_l^h(\mathbf{x}) = d^h(\mathbf{x}) \quad \mathbf{x} \in \Omega_l^h$$

and d^h as in (2.5). We rewrite this equation as follows

$$L_l^h U_l^h = f_l^h - L_\Gamma^h p_\Gamma r_\Gamma U^H + L_\Gamma^h(p_\Gamma U_\Gamma^H - U_\Gamma^h) + d_l^h.$$

Subtracting (3.3) from this equation yields (3.6). $\square$

From (3.6) it follows that the error vector $U_l^h - u_l^h$ can be divided into three parts:

$$U_l^h - u_l^h = e_l^h + E_l^h + \epsilon_l^h, \tag{3.8}$$

with

$$L_l^h e_l^h = d_l^h, \tag{3.9}$$

$$L_l^h E_l^h = -L_\Gamma^h (U_\Gamma^h - p_\Gamma U_\Gamma^H), \tag{3.10}$$

$$L_l^h \epsilon_l^h = -L_\Gamma^h p_\Gamma r_\Gamma (U^H - u^H). \tag{3.11}$$

We do not expect that cancellation effects occur in the right hand side of (3.8).
Since $d_l^h(\mathbf{x}) = d^h(\mathbf{x})$ at all $\mathbf{x} \in \Omega_l^h$ we have that

$$\|e_l^h\|_\infty \leq c \|U^h - u^h\|_\infty,$$

with $c \approx 1$ independent of h. Discrete problems (3.10) and (3.11) are related to the homogeneous partial differential equation

$$\mathcal{L}V = 0 \quad \text{on } \Omega_l$$

with homogeneous Dirichlet boundary conditions on $\partial\Omega_l \cap \partial\Omega$ and inhomogeneous Dirichlet boundary conditions on Γ. They result from discretization of this partial differential equation on Ω_l^h. Suppose that a discrete maximum-minimum principle holds for these problems. Then the errors E_l^h and ϵ_l^h satisfy

$$\begin{aligned} \|E_l^h\|_\infty &\leq \|U_\Gamma^h - p_\Gamma U_\Gamma^H\|_\infty, \\ \|\epsilon_l^h\|_\infty &\leq \|r_\Gamma (U^H - u^H)\|_\infty. \end{aligned}$$

If the order of the interpolation operator p_Γ is high enough, we have that

$$\|U_\Gamma^h - p_\Gamma U_\Gamma^H\|_\infty \leq \|U^h - u^h\|_\infty$$

and thus

$$\|E_l^h\|_\infty \leq \|U^h - u^h\|_\infty.$$

Usually linear interpolation suffices, because U is assumed to behave smoothly near the interface Γ.
From the definition of r_Γ it follows that

$$\|r_\Gamma (U^H - u^H)\|_\infty = \max_{\mathbf{x} \in \Gamma^H} |U^H(\mathbf{x}) - u^H(\mathbf{x})| =: \|U^H - u^H\|_{\infty, \Gamma^H}.$$

Now the following estimate of $\|U_l^h - u_l^h\|_\infty$ results

$$\|U_l^h - u_l^h\|_\infty \leq \|U^H - u^H\|_{\infty, \Gamma^H} + (c+1) \|U^h - u^h\|_\infty, \tag{3.12}$$

with $c \approx 1$. So the accuracy of the solution of the local fine grid problem (3.3) depends on how accurate the global coarse grid approximation u^H is on the interface Γ.

From the definition of u^c in (3.4) it follows that

$$\|U^c - u^c\|_\infty = \max\{\|U^H - u^H\|_{\infty, \Omega^H \setminus \Omega_l}, \|U_l^h - u_l^h\|_\infty\}, \tag{3.13}$$

where

$$\|w^H\|_{\infty,\Omega^H\setminus\Omega_l} := \max_{\mathbf{x}\in\Omega^H\setminus\Omega_l} |w^H(\mathbf{x})|.$$

Since $\Gamma^H \subset \Omega^H\setminus\Omega_l$ we have from (3.12) and (3.13) that

$$\|U^c - u^c\|_\infty \leq \|U^H - u^H\|_{\infty,\Omega^H\setminus\Omega_l} + (c+1)\|U^h - u^h\|_\infty. \tag{3.14}$$

From Theorem 3.2 it is clear that the error $\|U^H - u^H\|_{\infty,\Omega^H\setminus\Omega_l}$ depends on the local discretization error d^H. We recall that $|d^H|$ has a very typical behaviour: at several grid points $\mathbf{x}$ inside Ω_l the error $|d^H(\mathbf{x})|$ is much larger than at grid points outside Ω_l. For some problems the error $|U^H(\mathbf{y}) - u^H(\mathbf{y})|$ is small whenever the local discretization error $|d^H(\mathbf{y})|$ is small. In general, however, this is not true. The inverse operator $(L^H)^{-1}$ may *spread local effects* over a large part of the domain. For the one dimensional Poisson problem with central difference discretization $(L^H)^{-1}$ is known and the *spreading effect* is illustrated in the following examples.

Example 3.4
Consider the one dimensional Poisson problem (2.2) from Example 2.1. Discretization on Ω^H yields the finite difference matrix

$$L^H = \frac{1}{H^2}\begin{pmatrix} 2 & -1 & & & \\ -1 & 2 & -1 & & \\ & & \ddots & & \\ & & -1 & 2 & -1 \\ & & & -1 & 2 \end{pmatrix} \in I\!R^{M\times M}$$

with $H = 1/(M+1)$.
The coefficients of $(L^H)^{-1}$ are given by

$$((L^H)^{-1})_{i,j} = \begin{cases} H^3\,(M+1-i)\,j & j \leq i \\ H^3\,(M+1-j)\,i & j > i \end{cases}.$$

Suppose that the components of d^H are given by

$$(d^H)_j = \begin{cases} K & j = l \\ 0 & j \neq l \end{cases}, 1 \leq l \leq M,$$

with $K > tol/(\min\{l, M+1-l\}H^3)$.
Then we get

$$((L^H)^{-1}d^H)_i = \begin{cases} i\,(M+1-l)\,K\,H^3 & 1 \leq i < l \leq M \\ (M+1-i)\,l\,K\,H^3 & M \geq i \geq l \geq 1 \end{cases}.$$

The largest component of this vector occurs for $i = l$. A linear reduction holds for the other components. The smallest component is reached for $i = 1$ or $i = M$. We have that

$$(L^H)^{-1}d^H(\mathbf{x}) \geq \min\{l, M+1-l\}\,H^3\,K > tol.$$

So we see that all components of $(L^H)^{-1}d^H$ are relatively large, although almost all components of d^H are equal to zero. □

Example 3.5
Consider the one dimensional Poisson problem from Example 2.1:

$$-U_{xx} = A^2 \frac{\tanh(A(x-z))}{\cosh^2(A(x-z))} \quad 0 < x < 1 \tag{3.15}$$

with Dirichlet boundary conditions.
The continuous solution is given by

$$U(x) = (\tanh(A(x-z)) + 1)/2.$$

We discretize on a uniform grid with grid size $H = 1/16$ using central differences. In Figure 6

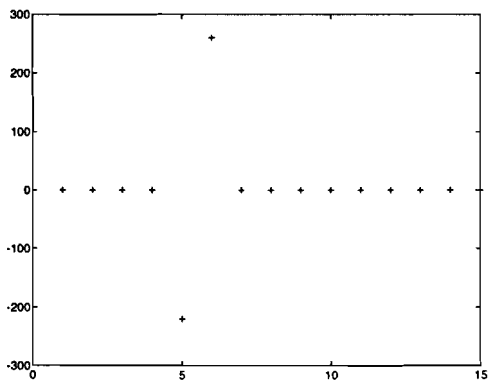

Figure 6: Local discretization error for (3.15) with $A = 200$ and $z = 0.333$.

the local discretization error d^H is presented for problem (3.15) with $A = 200$ and $z = 0.333$. At the grid points $x_5 = 5/16$ and $x_6 = 6/16$ the absolute value of the local discretization error is much larger than at the other grid points. If we consider the local discretization error, a reasonable choice for the refinement region Ω_l seems to be $\Omega_l = (3/16, 8/16)$. In Figure 7

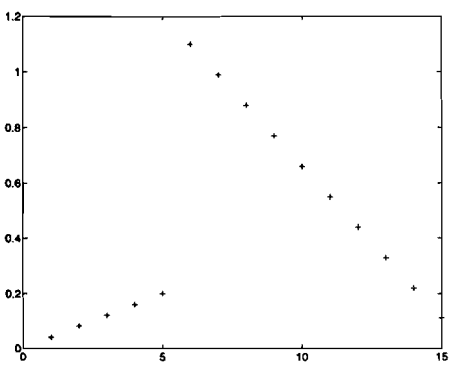

Figure 7: Global error $|U^H(x) - u^H(x)|$ for (3.15) with $A = 200$ and $z = 0.333$.

the global error $|U^H(x) - u^H(x)|$ is shown. We see that at the grid points $x_3 = 3/16$ and $x_8 = 8/16$ this error is still ≈ 1, although the local discretization error at these grid points is $\approx 10^{-4}$. □

Example 3.6
Consider the one dimensional convection-diffusion problem

$$-\epsilon U_{xx} + U_x = \frac{2\tanh(\frac{x-z}{\epsilon}) + 1}{2\epsilon \cosh^2(\frac{x-z}{\epsilon})} \quad 0 < x < 1, \tag{3.16}$$

with Dirichlet boundary conditions. The continuous solution is given by

$$U(x) = (\tanh(\frac{x-z}{\epsilon}) + 1)/2.$$

The diffusion term is discretized using a central difference scheme. The convection term using a first order upwind scheme. We discretize on a uniform grid with grid size $H = 1/16$. In Figure 8 and Figure 9 the local discretization error and the error $|U^H(x) - u^H(x)|$ are presented for $\epsilon = 0.01$ and $x = 0.5$. The local discretization error $|d^H|$ has a few large components near z. At grid points away from z (e.g. $x \geq 11/16$) this error is very small ($\approx 10^{-5}$). The global error $|U^H(x) - u^H(x)|$ also reaches its maximum value at a grid point near z. At grid points $x > z$ this error hardly decreases. For grid points $x \geq 11/16$ we still have $|U^H(x) - u^H(x)| \approx 5$. □

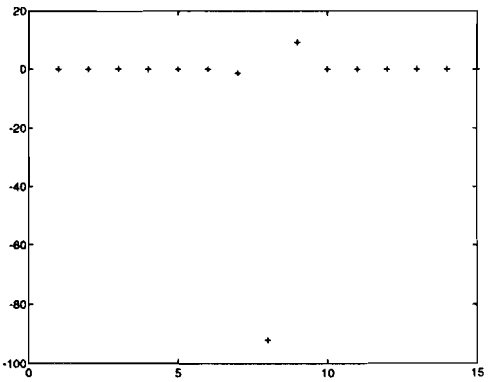

Figure 8: Local discretization error for (3.16) with $\epsilon = 0.01$ and $z = 0.5$.

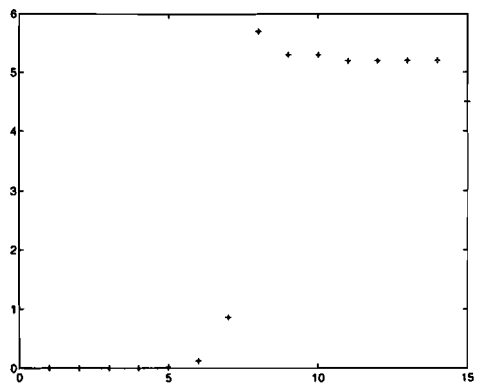

Figure 9: Global error $|U^H(x) - u^H(x)|$ for (3.16) with $\epsilon = 0.01$ and $z = 0.5$.

From (3.14) we have that the accuracy of the approximation u^c from (3.4), which is measured by $\|U^c - u^c\|_\infty$, depends on two terms: $\|U^H - u^H\|_{\infty,\Omega^H \setminus \Omega_l}$ and $\|U^h - u^h\|_\infty$. Clearly we cannot expect that u^c is more accurate than the global fine grid approximation and in general $\|U^H - u^H\|_{\infty,\Omega^H \setminus \Omega_l}$ is the dominant term:

$$\|U^c - u^c\|_\infty \approx \|U^H - u^H\|_{\infty,\Omega^H \setminus \Omega_l}.$$

We have seen that

$$\|U^H - u^H\|_{\infty,\Omega^H \setminus \Omega_l} \approx \sigma \|U^H - u^H\|_\infty$$

where $0 < \sigma < 1$ depends on the spreading effect of $(L^H)^{-1}$. If σ is close to 1 (which is the case in Example 3.5 and Example 3.6), then the accuracy of u^c is comparable to the accuracy of the global coarse grid approximation. So despite the fact that the grid sizes that are used in the discretization process are in agreement with the behaviour of the continuous solution (see (2.11)), the accuracy of the resulting approximation is not in agreement with the grid sizes that are used. The reason is that the accuracy of the approximation u^c depends on components of $|d^H|$ at grid points *inside* Ω_l (which are much larger than components of $|d^h|$ at grid points inside Ω_l).

4 Local Defect Correction Approach

In the local defect correction approach the approximation u_l^h (from (3.3)) is used to update the global coarse grid problem (3.1). The right hand side of (3.1) is updated at grid points that are part of a *local coarse subgrid* Ω_s^H. This is a uniform grid with grid size H that covers a region $\Omega_s \subseteq \Omega_l$. The interface between Ω_s and Ω is denoted by Γ_s (see Figure 9). We

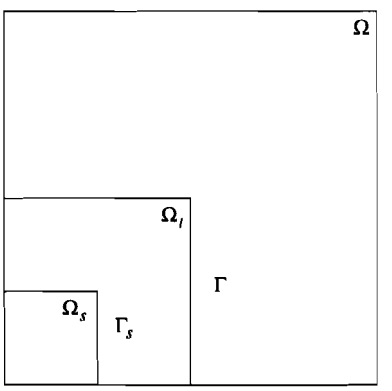

Figure 10: Example of the regions Ω, Ω_l, and Ω_s in $\mathbb{R}^2$.

assume that this interface Γ_s coincides with grid points of Ω^H in the one dimensional case and with grid lines of Ω^H in the two dimensional case. We also assume that the distance between a point on Γ_s and Γ is constant. We define:

$$dist := \min\{|\mathbf{x} - \mathbf{y}| \; | \mathbf{x} \in \Gamma_s, \; \mathbf{y} \in \Gamma\}. \tag{4.1}$$

If $dist = 0$ then $\Omega_s = \Omega_l$, $\Gamma_s = \Gamma$, and $\Omega_s^H = \Omega_l^H$. The *local coarse grid* Ω_l^H is a uniform grid with grid size H that covers the local region Ω_l.

The updated global coarse grid problem is given by

$$L^H \bar{u}^H = \bar{f}^H \tag{4.2a}$$

with

$$\bar{f}^H(\mathbf{x}) := \begin{cases} (L_l^H r_l u_l^h)(\mathbf{x}) + (L_\Gamma^H r_\Gamma u^H)(\mathbf{x}) & \mathbf{x} \in \Omega_s^H \\ f^H(\mathbf{x}) & \mathbf{x} \in \Omega^H \backslash \Omega_s^H \end{cases} . \tag{4.2b}$$

The operators L_l^H and L_Γ^H result from finite difference discretization of (2.1) on Ω_l^H; they are the coarse grid analogues of L_l^h and L_Γ^h from (3.3). In this discretization process the same finite difference scheme is used as in the discretization process on the global coarse grid:

$$(L^H w^H)(\mathbf{x}) = (L_l^H w_l^H)(\mathbf{x}) + (L_\Gamma^H w_\Gamma^H)(\mathbf{x}) \quad \mathbf{x} \in \Omega_l^H \tag{4.3}$$

for all grid functions w^H, w_l^H, and w_Γ^H that satisfy

$$\begin{aligned} w_l^H(\mathbf{x}) &= w^H(\mathbf{x}) \qquad \mathbf{x} \in \Omega_l^H, \\ w_\Gamma^H(\mathbf{x}) &= w^H(\mathbf{x}) \qquad \mathbf{x} \in \Gamma^H. \end{aligned}$$

The *trivial injection* r_l is used to restrict grid functions defined on Ω_l^h to Ω_l^H:

$$(r_l u_l^h)(\mathbf{x}) = u_l^h(\mathbf{x}) \quad \mathbf{x} \in \Omega_l^H.$$

The restriction r_Γ has been defined in (3.2).
We define the characteristic function χ by

$$\chi w(\mathbf{x}) := \begin{cases} w(\mathbf{x}) & \mathbf{x} \in \Omega_s^H \\ 0 & \mathbf{x} \in \Omega^H \backslash \Omega_s^H \end{cases} . \tag{4.4}$$

Then we can rewrite (4.2a), (4.2b) as follows:

$$L^H \bar{u}^H = f^H + \chi(L_l^H r_l u_l^h + L_\Gamma^H r_\Gamma u^H - f^H). \tag{4.5}$$

So the right hand side of the global coarse grid problem is *corrected* by the *defect* of a *local* fine grid approximation. (Hence the name *local defect correction approach*). Once we have solved (4.5) we can update the local fine grid problem :

$$L_l^h \bar{u}_l^h = f_l^h - L_\Gamma^h p_\Gamma r_\Gamma \bar{u}^H. \tag{4.6}$$

From the local defect correction approach the following approximation on the composite grid Ω^c results:

$$\bar{u}^c(\mathbf{x}) := \begin{cases} \bar{u}_l^h(\mathbf{x}) & \mathbf{x} \in \Omega_l^h \\ \bar{u}^H(\mathbf{x}) & \mathbf{x} \in \Omega^c \backslash \Omega_l^h \end{cases} . \tag{4.7}$$

In order to obtain this approximation we have to solve two discrete problems on the global coarse grid and two discrete problems on the local fine grid. We note that $(\bar{u}^H, \bar{u}_l^h)$ is equal to the first iterate in the local defect correction iteration by Hackbusch ([5],[6]).

The accuracy of $\bar{u}^c$ depends on the accuracy of $\bar{u}^H$ at grid points outside Ω_l and on the accuracy of $\bar{u}_l^h$ at grid points inside Ω_l. For the error $U_l^h - \bar{u}_l^h$ a similar expression holds as for the error $U_l^h - u_l^h$ (see Theorem 3.3).

Theorem 4.1
The approximation $\bar{u}_l^h$ that resuls from (4.6) satisfies

$$L_l^h(U_l^h - \bar{u}_l^h) = d_l^h + L_\Gamma^h(p_\Gamma U_\Gamma^H - U_\Gamma^h) - L_\Gamma^h p_\Gamma r_\Gamma(U^H - \bar{u}^H), \tag{4.8}$$

with

$$d_l^h(\mathbf{x}) = d^h(\mathbf{x}) \quad \mathbf{x} \in \Omega_l^h$$

and d^h as in (2.5).
Proof:
Analogous to the proof of Theorem 3.3. □

Equation (4.8) is very similar to (3.6). The only difference is that on the right hand side of (4.8) the error $U^H - \bar{u}^H$ is involved instead of $U^H - u^H$. We have (cf. (3.12), (3.14))

$$\|U_l^h - \bar{u}_l^h\|_\infty \leq \|U^H - \bar{u}^H\|_{\infty,\Gamma^H} + (c+1)\|U^h - u^h\|_\infty, \tag{4.9}$$

$$\|U^c - \bar{u}^c\|_\infty \leq \|U^H - \bar{u}^H\|_{\infty,\Omega^H\setminus\Omega_l} + (c+1)\|U^h - u^h\|_\infty, \tag{4.10}$$

with $c \approx 1$. Thus $\|U^c - \bar{u}^c\|_\infty$ depends on $|U^H(\mathbf{x}) - \bar{u}^H(\mathbf{x})|$ at grid points $\mathbf{x} \in \Omega^H\setminus\Omega_l$.

Theorem 4.2
The approximation $\bar{u}^H$ that resuls from (4.5) satisfies

$$\begin{aligned} L^H(U^H - \bar{u}^H) = {} & (1-\chi)d^H + \chi L_l^H r_l (L_l^h)^{-1} d_l^h + \chi L_l^H r_l (L_l^h)^{-1} L_\Gamma^h (p_\Gamma U_\Gamma^H - U_\Gamma^h) \\ & + \chi(L_\Gamma^H - L_l^H r_l (L_l^h)^{-1} L_\Gamma^h p_\Gamma) r_\Gamma (U^H - u^H). \end{aligned} \tag{4.11}$$

Proof:
From (2.10), (4.3), and (4.4) we have that

$$L^H U^H = f^H + \chi(L_l^H U_l^H + L_\Gamma^h U_\Gamma^H - f^H) + (1-\chi)d^H.$$

Combination of this equation with (4.5) yields

$$L^H(U^H - \bar{u}^H) = \chi(L_l^H r_l(U_l^h - u_l^h) + L_\Gamma^H r_\Gamma(U^H - u^H)) + (1-\chi)d^H.$$

From Theorem 3.3 we have

$$U_l^h - u_l^h = (L_l^h)^{-1} d_l^h + (L_l^h)^{-1} L_\Gamma^h (p_\Gamma U_\Gamma^H - U_\Gamma^h) - (L_l^h)^{-1} L_\Gamma^h p_\Gamma r_\Gamma (U^H - u^H).$$

Using this we get

$$\begin{aligned} L^H(U^H - \bar{u}^H) = {} & (1-\chi)d^H + \chi L_l^H r_l (L_l^h)^{-1} d_l^h + \\ & \chi(L_\Gamma^H - L_l^H r_l (L_l^h)^{-1} L_\Gamma^h p_\Gamma) r_\Gamma (U^H - u^H) + \chi L_l^H r_l (L_l^h)^{-1} L_\Gamma^h (p_\Gamma U_\Gamma^H - U_\Gamma^h). \end{aligned}$$

□

We note that for one dimensional problems the third term on the right hand side of (4.11) is equal to zero, because in the one dimensional case we have $\Gamma^H = \Gamma^h$. In the case of a one dimensional Poisson problem with a central difference discretization the fourth term on the right hand side of (4.11) also equals zero. In this case the approximation $(\bar{u}^H, \bar{u}_l^h)$ from (4.5), (4.6) is equal to the limit value of the local defect correction iteration that is described in [5], [6]. This also holds if instead of the trivial restriction another restriction r_l is used.

The effect of the local defect correction approach is illustrated by some numerical examples.

Example 4.3
Consider the one dimensional Poisson problem from Example 2.1 with $A = 100$ and $z = 0.4$. Let the coarse grid size be fixed: $H = 1/32$. Let the local region be given by $\Omega_l = (10/32, 16/32)$ and let $dist = 0$ (see (4.1)). In Table 1 the errors $\|U^H - \bar{u}^H\|_\infty$, $\|U^H - \bar{u}^H\|_{\infty,\Omega^H\setminus\Omega_l}$, $\|U_l^h - \bar{u}_l^h\|_\infty$, and $\|U^h - u^h\|_\infty$ are presented for different grid sizes h. The error $\|U^c - \bar{u}^c\|_\infty$ is equal to the maximum of the numbers in the third and fourth column

h	$\|U^H - \bar{u}^H\|_\infty$	$\|U^H - \bar{u}^H\|_{\infty,\Omega^H\setminus\Omega_l}$	$\|U_l^h - \bar{u}_l^h\|_\infty$	$\|U^h - u^h\|_\infty$
$1/32$			$2.7e+01$	
$1/64$	$2.7e+00$	$2.2e+00$	$2.7e+00$	$2.7e+00$
$1/128$	$2.9e-02$	$2.5e-02$	$4.7e-02$	$4.7e-02$
$1/256$	$5.1e-03$	$7.3e-05$	$5.1e-03$	$5.0e-03$
$1/512$	$1.3e-03$	$7.6e-05$	$1.3e-03$	$1.2e-03$
$1/1024$	$3.7e-04$	$7.7e-05$	$3.7e-04$	$3.1e-04$
$1/2048$	$1.4e-04$	$7.7e-05$	$1.4e-04$	$7.6e-05$

Table 1: Results for Example 4.3.

of Table 1. We see that for this example we always have $\|U^c - \bar{u}^c\|_\infty = \|U_l^h - \bar{u}_l^h\|_\infty$. The numbers in Table 1 indicate that the accuracy of $\bar{u}^c$ is comparable to the accuracy of the *global fine grid approximation* u^h for this model problem. The approximation u^c that results from the first approach (see Section 3) satisfies $\|U^c - u^c\|_\infty = 2.2e+01$. Thus the accuracy of u^c is comparable to the accuracy of the *global coarse grid approximation* u^H. The numbers in the second column of Table 1 indicate that also the accuracy of $\bar{u}^H$ is comparable to the accuracy of the global fine grid approximation. We see that $\|U^H - \bar{u}^H\|_{\infty,\Omega^H\setminus\Omega_l} \ll \|U^H - \bar{u}^H\|_\infty$ for several values of h. Probably this is due to cancellation effects. We note that these cancellation effects do not *essentially* improve the resulting local defect correction approximation. Finally we note that the results obtained with the local defect correction approach with $dist > 0$ are not as good as the results obtained for $dist = 0$. □

For other one dimensional problems (e.g. convection-diffusion problems) the fourth term on the right hand side of (4.11) is not equal to zero. In this case $(\bar{u}^H, \bar{u}_l^h)$ is not equal to the limit value of the local defect correction iteration in [5].

Example 4.4
Consider the one dimensional convection diffusion problem

$$-U_{xx} - U_x = \frac{A^2 \tanh(A(x - x_0)) - A/2}{\cosh^2(A(x - x_0))}, \quad 0 < x < 1,$$

with Dirichlet boundary conditions such that the continuous solution is given by

$$U(x) = \frac{\tanh(A(x - x_0)) + 1}{2}.$$

Let $A = 100$ and $x_0 = 0.4$. Let the coarse grid size be fixed: $H = 1/32$. Let the local region be given by $\Omega_l = (10/32, 16/32)$ and let $dist = 0$. Both the convection and diffusion term are discretized using central differences. In Table 2 the errors $\|U^H - \bar{u}^H\|_{\infty,\Omega^H \setminus \Omega_l}$, $\|U_l^h - \bar{u}_l^h\|_\infty$, and $\|U^h - u^h\|_\infty$ are presented for different grid sizes h. The error $\|U^c - \bar{u}^c\|_\infty$ is equal to the

h	$\|U^H - \bar{u}^H\|_{\infty,\Omega^H \setminus \Omega_l}$	$\|U_l^h - \bar{u}_l^h\|_\infty$	$\|U^h - u^h\|_\infty$
$1/32$			$2.6e+01$
$1/64$	$2.1e+00$	$2.7e+00$	$2.7e+00$
$1/128$	$2.4e-02$	$4.7e-02$	$4.7e-02$
$1/256$	$8.1e-05$	$5.1e-03$	$5.0e-03$
$1/512$	$8.5e-05$	$1.3e-03$	$1.2e-03$

Table 2: Results for Example 4.4.

maximum of the numbers in the second and third column of Table 2. We note that for the approximation u^c that results from the first approach the following holds

$$\|U^c - u^c\|_\infty = 2.2e+01.$$

So, the accuracy of u^c is comparable to the accuracy of the *global coarse grid approximation* u^H, while the accuracy of $\bar{u}^c$ is comparable to the accuracy of the *global fine grid approximation* u^h for this convection-diffusion model problem. As in Example 4.3 the results of the local defect correction approach with $dist > 0$ are not as good as those obtained for $dist = 0$. □

Next we consider an example for which the local defect correction approach with $dist > 0$ yields better results than the local defect correction approach with $dist = 0$.

Example 4.5
Consider the one dimensional convection-diffusion problem (see also Example 3.6)

$$-\epsilon U_{xx} + U_x = \frac{2\tanh(\frac{x-x_0}{\epsilon}) + 1}{2\epsilon \cosh^2(\frac{x-x_0}{\epsilon})} \quad 0 < x < 1,$$

with Dirichlet boundary conditions such that the continuous solution is given by

$$U(x) = \frac{\tanh(\frac{x-x_0}{\epsilon}) + 1}{2}.$$

dist	$\|U^H - \bar{u}^H\|_{\infty,\Omega^H\setminus\Omega_l}$	$\|U_l^h - \bar{u}_l^h\|_\infty$
0	$3.01e-01$	$2.55e-01$
H	$1.82e-02$	$3.24e-02$
$2H$	$7.62e-02$	$6.19e-02$

Table 3: Results for Example 4.5.

Let $x_0 = 0.4$ and $\epsilon = 1.0e-02$. In this case we have a convection dominated problem. Let $H = 1/32$, $\Omega_l = (10/32, 16/32)$, and $h = 1/512$. The convection term is discretized using upwind discretization. In Table 3 the errors $\|U^H - \bar{u}^H\|_{\infty,\Omega^H\setminus\Omega_l}$ and $\|U_l^h - \bar{u}_l^h\|_\infty$ are presented for several values of d. For this model problem we have $\|U^h - u^h\|_\infty = 3.24e-02$. In this case the local defect correction approach with $dist = H$ yields a much better approximation than the local defect correction approach with $dist = 0$. A further increase of *dist* does not yield a better result. An explanation of this phenomenon is given later on. □

The first and second term on the right hand side of (4.11) involve local discretization error vectors that are related to boundary value problem (2.1). The third and fourth term on the right hand side of (4.11) can also be expressed using local discretization error vectors. For the third term on the right hand side of (4.11) we introduce the following Dirichlet boundary value problem with zero right hand side:

$$\begin{aligned} \mathcal{L}V &= 0 \quad \text{in } \Omega_l \\ V &= g_v \quad \text{on } \Gamma \\ V &= 0 \quad \text{on } \partial\Omega_l\setminus\Gamma \end{aligned} \tag{4.12}$$

with

$$g_v(\mathbf{x}) = U(\mathbf{x}) - (p_\Gamma U_\Gamma^H)(\mathbf{x}) \quad \mathbf{x} \in \Gamma. \tag{4.13}$$

Here we consider $p_\Gamma U_\Gamma^H$ as an interpolation *function* on Γ. Discretization of this boundary value problem with respect to Ω_l^H yields

$$L_l^H v_l^H = 0 \tag{4.14}$$

since

$$g_v(\mathbf{x}) = 0 \quad \text{at all } \mathbf{x} \in \Gamma^H.$$

Discretization with respect to Ω_l^h yields

$$L_l^h v_l^h + L_\Gamma^h(U_\Gamma^h - p_\Gamma U_\Gamma^H) = 0 \tag{4.15}$$

since

$$g_v(\mathbf{x}) = (U_\Gamma^h - p_\Gamma U_\Gamma^H)(\mathbf{x}) \quad \mathbf{x} \in \Gamma^h.$$

The local discretization errors d_v^H and d_v^h are defined by

$$d_v^H := L_l^H V_l^H \tag{4.16}$$

and

$$d_v^h := L_l^h V_l^h + L_\Gamma^h(U_\Gamma^h - p_\Gamma U_\Gamma^H). \tag{4.17}$$

Here V_l^H (resp. V_l^h) is the restriction of the continuous solution of (4.12) to Ω_l^H (resp. Ω_l^h). The third term on the right hand side of (4.11) is rewritten using these local discretization error vectors.

Lemma 4.6

$$L_l^H r_l (L_l^h)^{-1} L_\Gamma^h (p_\Gamma U_\Gamma^H - U_\Gamma^h) = d_v^H - L_l^H r_l (L_l^h)^{-1} d_v^h. \tag{4.18}$$

Proof:
From (4.15) we have

$$(L_l^h)^{-1} L_\Gamma^h (p_\Gamma U_\Gamma^H - U_\Gamma^h) = v_l^h.$$

Thus

$$L_l^H r_l (L_l^h)^{-1} L_\Gamma^h (p_\Gamma U_\Gamma^H - U_\Gamma^h) = L_l^H r_l v_l^h.$$

Using (4.16) we get

$$\begin{aligned} L_l^H r_l v_l^h &= L_l^H r_l (v_l^h - V_l^h + V_l^h) \\ &= L_l^H V_l^H - L_l^H r_l (V_l^h - v_l^h) \\ &= d_v^H - L_l^H r_l (L_l^h)^{-1} L_l^h (V_l^h - v_l^h). \end{aligned}$$

From (4.15) and (4.17) we have

$$L_l^h (V_l^h - v_l^h) = d_v^h.$$

Using this we get

$$L_l^H r_l v_l^h = d_v^H - L_l^H r_l (L_l^h)^{-1} d_v^h.$$

□

For the fourth term on the right hand side of (4.11) we introduce the following Dirichlet boundary value problem:

$$\begin{aligned} \mathcal{L}W &= 0 \quad \text{in } \Omega_l \\ W &= g_w \quad \text{on } \Gamma \\ W &= 0 \quad \text{on } \partial\Omega_l \backslash \Gamma \end{aligned} \tag{4.19}$$

with

$$g_w(\mathbf{x}) = (p_\Gamma r_\Gamma (U^H - u^H))(\mathbf{x}) \quad \mathbf{x} \in \Gamma. \tag{4.20}$$

Here we consider $p_\Gamma r_\Gamma (U^H - u^H)$ as an interpolation *function* on Γ. Discretization of (4.19) with respect to Ω_l^H yields

$$L_l^H w_l^H + L_\Gamma^H r_\Gamma (U^H - u^H) = 0 \tag{4.21}$$

since

$$g_w(\mathbf{x}) = (U^H - u^H)(\mathbf{x}) \quad \mathbf{x} \in \Gamma^H.$$

Discretization of (4.19) with respect to Ω_l^h yields

$$L_l^h w_l^h + L_\Gamma^h p_\Gamma r_\Gamma (U^H - u^H) = 0 \tag{4.22}$$

since

$$g_w(\mathbf{x}) = p_\Gamma r_\Gamma (U^H - u^H)(\mathbf{x}) \quad \mathbf{x} \in \Gamma^h.$$

The local discretization errors d_w^H and d_w^h are defined by

$$d_w^H := L_l^H W_l^H + L_\Gamma^H r_\Gamma (U^H - u^H) \tag{4.23}$$

and

$$d_w^h := L_l^h W_l^h + L_\Gamma^h p_\Gamma r_\Gamma (U^H - u^H). \tag{4.24}$$

Here W_l^H (resp. W_l^h) is the restriction of the continuous solution of (4.19) to Ω_l^H (resp. Ω_l^h). The fourth term on the right hand side of (4.11) is rewritten using these local discretization error vectors.

Lemma 4.7

$$(L_\Gamma^H - L_l^H r_l (L_l^h)^{-1} L_\Gamma^h p_\Gamma) r_\Gamma (U^H - u^H) = d_w^H - L_l^H r_l (L_l^h)^{-1} d_w^h \tag{4.25}$$

Proof:
Since

$$L_\Gamma^H r_\Gamma (U^H - u^H) = -L_l^H w_l^H$$

and

$$L_\Gamma^h p_\Gamma r_\Gamma (U^H - u^H) = -L_l^h w_l^h$$

we have that

$$\begin{aligned}
(L_\Gamma^H - L_l^H r_l (L_l^h)^{-1} L_\Gamma^h p_\Gamma) r_\Gamma (U^H - u^H) &= L_l^H r_l w_l^h - L_l^H w_l^H \\
&= L_l^H r_l w_l^h - L_l^H W_l^H + L_l^H W_l^H - L_l^H w_l^H \\
&\overset{(4.23)}{=} L_l^H r_l (w_l^h - W_l^h) + d_w^H \\
&= d_w^H - L_l^H r_l (L_l^h)^{-1} L_l^h (W_l^h - w_l^h) \\
&\overset{(4.22,4.24)}{=} d_w^H - L_l^H r_l (L_l^h)^{-1} d_w^h
\end{aligned}$$

□

Now the right hand side of (4.11) can be expressed using local discretization error vectors only.

Theorem 4.8
The approximations $\bar{u}^H$ and $\bar{u}_l^h$ that result from (4.5) and (4.6) satisfy

$$\begin{aligned}
L^H (U^H - \bar{u}^H) &= (1-\chi) d^H + \chi L_l^H r_l (L_l^h)^{-1} d_l^h \\
&\quad + \chi d_v^H + \chi d_w^H \\
&\quad - \chi L_l^H r_l (L_l^h)^{-1} d_v^h - \chi L_l^H r_l (L_l^h)^{-1} d_w^h \qquad (4.26) \\
L_l^h (U_l^h - \bar{u}_l^h) &= d_l^h + L_\Gamma^h (p_\Gamma U_\Gamma^H - U_\Gamma^h) - L_\Gamma^h p_\Gamma r_\Gamma (U^H - \bar{u}^H). \qquad (4.27)
\end{aligned}$$

Proof:
This follows immediately from Theorem 4.1, Theorem 4.2, Lemma 4.6, and Lemma 4.7. □

We recall that the accuracy of the approximation $\bar{u}^c$ from (4.7) depends on the accuracy of $\bar{u}^H$ at grid points $\mathbf{x} \in \Omega^H \backslash \Omega_l$:

$$\|U^c - \bar{u}^c\|_\infty \leq \|U^H - \bar{u}^H\|_{\infty, \Omega^H \backslash \Omega_l} + (c+1) \|U^h - u^h\|_\infty.$$

The error $\|U^H - \bar{u}^H\|_{\infty,\Omega^H \backslash \Omega_l}$ depends on the size of the components on the right hand side of (4.26).

We compare (4.26) with (3.5). In Section 3 we have seen that the large components of $|d^H|$ at grid points inside Ω_l are the reason that, in general, the approximation u^c from (3.4) is only slightly more accurate than the global coarse grid approximation u^H. The first term on the right hand side of (4.26) only contains components of d^H that correspond to grid points outside Ω_s (see (4.4)). If Ω_s is large enough, i.e. if *dist* in (4.1) is small enough, then the large components of $|d^H|$ do not appear on the right hand side of (4.26). In the special case that *dist* = 0 we have from (2.11) that

$$\|(1-\chi)d^H\|_\infty \approx \|d^h\|_\infty.$$

On the right hand side of (4.26) five other terms appear. All these terms have zero components at grid points outside Ω_s (see (4.4)). The second term on the right hand side of (4.26) contains components of the local discretization error d^h (see (3.7)) that correspond to grid points inside Ω_l. These components are sufficiently small, since we have assumed that the grid size h is in agreement with the behaviour of the continuous solution inside Ω_l. These first two terms are in some way inevitable in a local defect correction approach. To show this we consider the following "ideal local defect correction approach". Suppose that the *global fine grid approximation* u^h from (2.4) is known. Then we can use the grid functions u_l^{*h} and u_Γ^{*H} that are given by

$$\begin{aligned} u_l^{*h}(\mathbf{x}) &= u^h(\mathbf{x}) \quad \mathbf{x} \in \Omega_l^h, \\ u_\Gamma^{*H}(\mathbf{x}) &= u^h(\mathbf{x}) \quad \mathbf{x} \in \Gamma^H, \end{aligned}$$

to correct the right hand side of the global coarse grid problem as in (4.5):

$$L^H u^{*H} = (1-\chi)f^H + \chi(L_l^H r_l u_l^{*h} + L_\Gamma^H u_\Gamma^{*H}).$$

For the error $U^H - u^{*H}$ we can derive the following expression:

$$\begin{aligned} L^H(U^H - u^{*H}) &= (1-\chi)d^H + \chi L_l^H r_l (L_l^h)^{-1} d_l^h \\ &\quad + \chi(L_\Gamma^H r_\Gamma - L_l^H r_l (L_l^h)^{-1} L_\Gamma^h)(U_\Gamma^h - u_\Gamma^{*h}) \end{aligned} \tag{4.28}$$

with

$$u_\Gamma^{*h}(\mathbf{x}) = u^h(\mathbf{x}) \quad \mathbf{x} \in \Gamma^h.$$

This expression is derived in a similar way as the expression in (4.11). The first two terms on the right hand side of (4.28) are the same as the first two terms on the right hand side of (4.26).

The third and fourth term on the right hand side of (4.26) involve local discretization error vectors d_v^H and d_w^H. These correspond to the boundary value probems (4.12) and (4.19) respectively and to the coarse grid size H. The size of the components of these local discretization error vectors depends on the behaviour of the continuous solutions V and W respectively. The Dirichlet boundary value problems in (4.12) and (4.19) both have the right hand side of the partial differential equation and the right hand side of the boundary condition on $\partial\Omega_l \backslash \Gamma$ equal to zero. We have assumed that the existence of the high activity region for the continuous solution U of (2.1) is due to the forcing term f or to the right hand side g in the Dirichlet boundary condition in (2.1). Therefore V and W have a much smoother behaviour inside Ω_l than U. On the interface Γ an inhomogeneous Dirichlet boundary condition is

prescribed. Derivatives of V and W can be large near the interface. For the one dimensional convection-diffusion problem in Example 4.5 we have

$$\begin{aligned} &-\epsilon W_{xx} + W_x = 0 \quad 10/32 < x < 16/32, \\ &W(10/32) = U(10/32) - u^H(10/32), \\ &W(16/32) = U(16/32) - u^H(16/32). \end{aligned}$$

For $\epsilon \ll 1$ this problem is strongly convection dominated. In general $W(10/32) \neq W(16/32)$ and then W varies very rapidly near the right interface point. Thus $|d_w^H|$ has relatively large components at grid points near the interface.

For two dimensional problems we have to interpolate Dirichlet boundary conditions on the interface. If a low order interpolation operator is used (e.g. linear interpolation), then $|d_v^H|$ and $|d_w^H|$ have relatively large components at grid points near the interface. (For higher order interpolation operators these local discretization errors are expected to become smaller). If Ω_s is small enough, i.e. if *dist* is large enough, then these large components are replaced by zero in χd_v^H and χd_w^H.

We note that an optimal choice for *dist* with respect to the third and fourth term on the right hand side of (4.26) (i.e. "*dist* is large") contradicts with the optimal choice for *dist* with respect to the first term on the right hand side of (4.26) (i.e. *dist* = 0). In general a small *dist* > 0 (e.g. *dist* = H, *dist* = $2H$) yields a satisfactory approximation $\bar{u}^c$ in the two dimensional case (see the numerical examples in [5]). For the one dimensional diffusion problem and the one dimensional convection-diffusion problem in Example 4.3 and Example 4.4 respectively the corresponding continuous solution W behaves smoothly near the interface and then the local defect correction approach with *dist* = 0 yields satisfactory results.

The fifth and sixth term on the right hand side of (4.26) are also related to the boundary value problems (4.12) and (4.19). These terms correspond to the *fine grid size h*. We have assumed that this grid size is in agreement with the behaviour of the continuous solution U from (2.1) inside the high activity region. We do not expect that derivatives of V and W are larger than corresponding derivatives of U in Ω_l. Then the fifth and sixth term on the right hand side of (4.26) are not larger than the second term on the right hand side of (4.26).

Concluding we can say that the accuracy of the local defect correction approximation u^c depends highly on the choice for *dist* in (4.1). For one dimensional problems the optimal choice for *dist* depends on the behaviour of the solution of the two point boundary value problem

$$\begin{aligned} \mathcal{L}W &= 0 && \text{in } \Omega_l, \\ W &= 0 && \text{on } \partial\Omega_l \backslash \Gamma, \\ W &= U^H - u^H && \text{on } \Gamma. \end{aligned}$$

If W behaves smoothly in Ω_l, then *dist* = 0 is a good choice (see Example 4.3 and Example 4.4). If W varies rapidly near the interface Γ (e.g. in case of a convection-diffusion problem with strong convection, see Example 4.5) the local defect correction approach with a small *dist* > 0 (e.g. *dist* = H) yields satisfactory results. In both cases the accuracy of the resulting approximation is comparable with the accuracy of the global fine grid approximation.

For two dimensional problems the choice for *dist* depends on the behaviour of the continuous solutions of the boundary value problems (4.12) and (4.19). The behaviour of these continuous solutions near the interface depends on the choice for the interpolation operator p_Γ. If a low order interpolation operator is used (e.g. linear interpolation, which is a practical

choice), then the continuous solutions of (4.12) and (4.19) have large derivatives near the interface. In this case the local defect correction approach with a small $dist > 0$ (e.g. $dist = H$) yields satisfactory results. The accuracy of the resulting approximation is comparable with the accuracy of the global fine grid approximation.

References

[1] Brandt, A.: *Multi-level adaptive solutions to boundary-value problems*, Math. Comp., 31 (1977), pp 333-390.

[2] Brandt, A.: *Multi-level adaptive techniques for singular-perturbation problems*, in Numerical Analysis of Singular Perturbation Problems, P.W. Hemker and J.J.H. Miller, eds, Academic Press, New York, 1979.

[3] Brandt, A.: *Multigrid techniques: 1984 guide with applications to fluid dynamics*, GMD-Studie No85, GMD, Sankt-Augustin, 1984.

[4] Brandt, A., Bai, D.: *Local mesh refinement multilevel techniques*, SIAM J. Sci. Stat. Comput., 8 (1987), pp 109-134.

[5] Hackbusch, W.: *Local defect correction method and domain decomposition techniques*, Computing, Suppl 5 (1984), pp 89-113.

[6] Hackbusch, W.: *Multigrid methods and applications*, Springer, Berlin, 1985.

[7] Larrouturou, B.: *A conservative adaptive method for flame propagation*, SIAM J. Sci. Stat. Comput., 10 (1989), pp 742-755.

[8] Mattheij, R.M.M., Smooke, M.D.: *Estimates for the inverse of tridiagonal matrices arising in boundary-value problems*, Linear Algebra Appl., 73 (1986), pp 33-57.

[9] Mc Cormick, S., Thomas, J.: *The fast adaptive composite grid (FAC) method for elliptic equations*, Math. Comp., 46 (1986), pp 439-456.

[10] Mc Cormick, S.F.: *Multilevel adaptive methods for partial differential equations*, SIAM, Philadelphia, 1989.

[11] Trompert, R.A.: *Local uniform grid refinement for time-dependent partial differential equations*, Ph.D. Thesis, Amsterdam University, Amsterdam, 1994.